

SOVIET PHYSICS

JETP

A translation of the Zhurnal Éksperimental'noi i Teoreticheskoi Fiziki.

Editor in Chief—P. L. Kapitza; *Associate Editors*—M. A. Leontovich, E. M. Lifshitz, S. Yu. Luk'yanov;

Editorial Board—É. L. Andronikashvili, K. P. Belov, V. P. Dzhelepov, E. L. Feinberg, V. A. Fock,

I. K. Kikoin, L. D. Landau, B. M. Pontecorvo, D. V. Shirkov, K. A. Ter-Martirosyan, G. V. Zhdanov (*Secretary*).

Vol. 25, No. 3, pp. 403-543

(Russ. Orig. Vol. 52, No. 3, pp. 617-831, March 1967)

September 1967

A STUDY OF THE FERMI SURFACE OF CADMIUM

V. P. NABEREZHNYKH, A. A. MAR'YAKHIN, and V. L. MEL'NIK

Donets Physico-technical Institute, Academy of Sciences, Ukrainian S.S.R.;

Physico-technical Low Temperature Institute, Academy of Sciences, Ukrainian S.S.R.

Submitted to JETP editor May 30, 1966

J. Exptl. Theoret. Phys. (U.S.S.R.) 52, 617-628 (March, 1967)

The Fermi surface of Cd is investigated by the rf size effect technique at 5 MHz and by the cyclotron resonance technique at 36 GHz in a magnetic field parallel to the surface of the sample. The experimental results are interpreted on the basis of a Fermi surface constructed in the almost free electron approximation. The most complete data have been obtained for the lens-shaped electron surface in the third zone, for the hole surface (the so-called "monster") in the second zone, and for the hole surface (pyramids) in the first zone. The shapes of some projections of the surfaces could be reconstructed from the experimental diameters. The largest deviations from the almost free electron model are observed for the hole surface in the second zone. This surface is open along the [0001] direction and consists of three fragments of the monster that are joined along the vertical edges of the Brillouin zone, thus forming a complex corrugated cylinder. The observed dimensions were considerably smaller than those based on the model. However, the shape and size of the lens-shaped electron surface in the third zone and of the hole surface in the first zone are not much different from those derived on the almost free electron model. Extremal diameters were also observed that may be ascribed to the greatly reduced electron surfaces of the "star" type in the third zone and of the "cigar" type in the fourth zone. However, due to the incompleteness of the data the shapes of the surfaces could not be determined.

INTRODUCTION

THE electron properties of cadmium have been studied in numerous publications. The Fermi surface of this metal has been investigated using the galvanomagnetic effect,^[1] the de Haas-van Alphen effect,^[2-4] the ultrasonic method,^[5,6] and cyclotron resonance.^[7,8]¹⁾ In most of these studies the

experimental results are interpreted on the basis of the almost free electron model.^[9] This approach is based on the fact that the direct construction of the surface from experimental data is not unique, and, since the data are incomplete, remains practically impossible, as a general rule. On the other hand, experiment has shown that the given model is a good first approximation for numerous metals such as Al, Pb, and In. The interpretation of experimental results is facilitated considerably thereby, and it becomes possible to distinguish the parts of the Fermi surface to which

¹⁾We are indebted to Professor R. G. Chambers for acquainting us with the dissertation of M. P. Shaw, and to Shaw, Eck, and Zych for a preprint of their article.

the model cannot be applied. Although this method of determining the shape of the Fermi surface has no adequate theoretical basis, the fruitfulness of the method becomes more and more obvious.

The Fermi surface of cadmium in the almost free electron approximation, with account taken of spin-orbit interactions leading to an energy gap on the hexagonal faces of the Brillouin zone, appears as a series of quite complex electron and hole surfaces located in the first to the fourth zones (Fig. 1). In the first zone, at each corner of a hexagonal face small hole parts are located in the form of two triangular pyramids connected at their bases. The experimental existence of these surfaces has been demonstrated by the de Haas-van Alphen effect.^[2-4]

In the second zone, according to the model, a multiply-connected hole surface is located (the monster), which when account is taken of spin-orbit coupling is found to be open along the [0001] direction. Indeed, the openness of this surface has been established from galvanomagnetic measurements,^[1] ultrasonics,^[10] and the size effect.^[11] The de Haas-van Alphen effect shows that the "arms of the monster" are broken along the [1120] direction and that the surface can be represented by three fragments of the monster that are joined along the vertical edges of the Brillouin zone. The results obtained for this surface indicate considerable deviations from the model; however, since only the cross sectional areas were measured, only very sparse exact quantitative data are available regarding these deviations. From the latest data on the de Haas-van Alphen effect^[4] it follows that the monster touches the vertical edges of the zone along their entire length, and a gap like that in Zn does not exist in Cd.

The most complete data have been obtained for the "lens-shaped" surface in the third zone. The ultrasonic, de Haas-van Alphen, and cyclotron resonance results indicate that the shape of this is very close to the model-based shape but is somewhat smaller than the latter. The third zone should contain, besides the "lenses," electron surfaces in the shape of "stars" on the horizontal edges along [1120], formed by intersections of two lenses. We still have no reliable experimental information about these surfaces; however, they must be quite large and are manifested in various effects. We also possess no experimental confirmation that there exist the aforementioned cigar-shaped surfaces located on the horizontal edges of the fourth zone along [1120] according to the model.

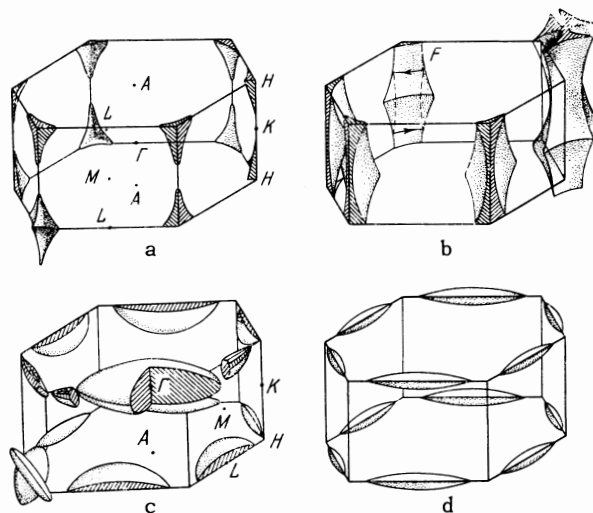


FIG. 1. Fermi surface of cadmium in the almost free electron model taking account of spin-orbit splitting and breaks in the arms of the monster. a—hole surfaces (pyramids) in the first Brillouin zone, b—hole surfaces consisting of fragments of the monster in the second zone, c—lens and star electron surfaces in the third zone, d—cigar-shaped electron surfaces in the fourth zone.

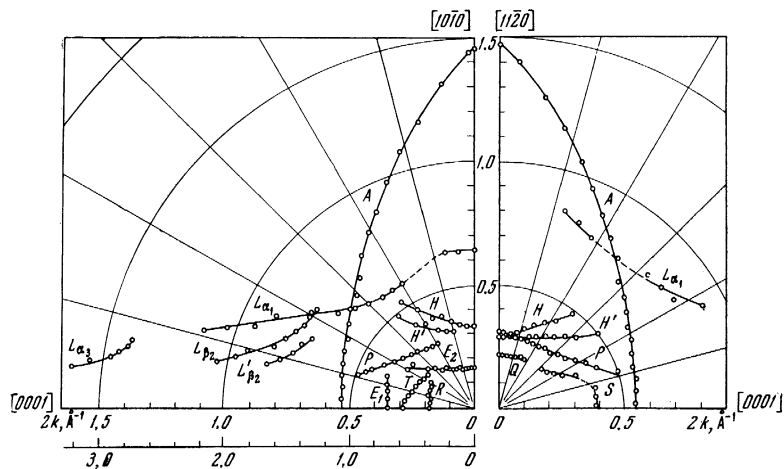
The previous investigations of the Fermi surface of Cd, although they give us much valuable information and indicate deviations of the surface from the almost free electron model, thus contain insufficient quantitative information concerning these deviations. We have therefore attempted to investigate the Fermi surface by the additional and comparatively new method of the rf size effect. This work was performed concomitantly with an investigation of cyclotron resonance in Cd, and the results obtained using the two different methods were interpreted from a single point of view. As previously, the interpretation was based on the almost free electron model.

The size effect experiments were performed at 5-MHz with a nuclear spectrometer. A Cd single crystal was placed horizontally inside an autodyne coil in such a way that it could be rotated with respect to the polarization of the rf current.

Cyclotron resonance was studied with a superheterodyne spectroscope at 36 GHz. The sample served as the bottom of a rectangular resonator in which an H_{012} wave was excited. The design of the resonator also permitted rotation of the sample about the polarization of the rf current. The angle of rotation of the sample about the magnetic direction was monitored in both experiments with an induction goniometer.^[12]

The magnetic field was generated by an electromagnet rotating in the horizontal plane. It was thus

FIG. 2. Anisotropy of maximal diameters of $2k$ orbits in the $(11\bar{2}0)$ and $(10\bar{1}0)$ planes measured by the size effect. The lower scale for the $(11\bar{2}0)$ plane pertains to the diameters L_{α_3} , L_{β_2} , and L_{β_2}' .



possible to register dR/dH for all orientations of the constant magnetic field and rf current about the crystallographic axes of the sample.

Cd samples were grown in a dismantlable glass mold by the method described in ^[13]. The initial material exhibited the following resistivity ratio at helium and room temperatures: $\rho(4.2^\circ\text{K})/\rho(300^\circ\text{K}) \approx (2-3) \times 10^{-5}$. The samples were disks with 12- and 8-mm diameters. In the size effect experiments we used samples with the following descriptions: $\mathbf{n} \parallel [11\bar{2}0]$, thicknesses 0.2 and 0.4 mm; $\mathbf{n} \parallel [0001]$, thicknesses 0.2 and 0.4 mm; $\mathbf{n} \parallel [10\bar{1}0]$, thickness 0.2 mm (\mathbf{n} is the normal to the surface of the sample). For cyclotron resonance we used 2-mm thick samples with $\mathbf{n} \parallel [11\bar{2}0]$, $\mathbf{n} \parallel [10\bar{1}0]$, and $\mathbf{n} \parallel [0001]$. The orientation was monitored by means of x rays. The deviation of the normal from the given directions did not exceed $1-2^\circ$. All measurements were obtained at 1.7°K .

EXPERIMENTAL RESULTS AND DISCUSSION

In the rf size effect experiments the maximal diameters of electron orbits are measured independently of the locations of any Fermi surfaces in Brillouin zones. The interpretation of the results is therefore very often hindered by extreme ambiguity. This pertains especially to orbits for which the projection of a Fermi surface in a given crystallographic plane has no center of symmetry. In Cd, where the Fermi surface is quite complex, this situation occurs very frequently. The angular dependences of the diameters then do not reflect the true shapes of Fermi surfaces and do not provide an intuitive picture.

Since the locations of the size effect lines were determined from the sharpest extremum of the derivative dR/dH , while the line shapes and their relative widths in some instances varied upon pro-

ceeding from one crystallographic plane to another, the given values of the wave vectors can contain systematic errors of the order of the relative line width.

THE LENS-SHAPED FERMI SURFACE IN THE THIRD ZONE

The strongest lines in both the size effect and cyclotron resonance are those due to lenses in the third zone. The size effect for all magnetic field directions except those close to symmetry axes are observed for both polarizations of the rf current: $\mathbf{J} \parallel \mathbf{H}$ and $\mathbf{J} \perp \mathbf{H}$; the intensity with $\mathbf{H} \parallel [10\bar{1}0]$ and $\mathbf{H} \parallel [11\bar{2}0]$ is 20 times greater than with $\mathbf{H} \parallel [0001]$. The extremal diameters for this surface are shown in Fig. 2 (denoted by A).

The experimental shape of a lens reproduces very well the shape obtained from the almost free electron model, although the size is somewhat smaller than for the latter. In the (0001) plane the size of the lens is constant at $2k = 1.46 \text{ \AA}^{-1}$, which gives the cross-sectional area $S = 1.7 \text{ \AA}^{-2}$. The same dimension according to ultrasonic measurements has been given as 1.56 \AA^{-1} ^[6] and 1.428 \AA^{-1} .^[5] Since these ultrasonic results differ by almost 10% from each other, a comparison based upon these is not decisive. The 10% difference between the area based on our data and on the de Haas-van Alphen effect is evidently associated with some systematic error resulting from ambiguity in determining the exact time of the orbital cutoff. Since the line shape is very complex in the size effect, and the line width was about 7%, an error of +5% is quite likely in registering the cutoff field from zero to the first extremum of a line.

Since the experimental shape of the lens surface agrees well with the model at the $[0001]$ axis, an attempt was made, using the method of least

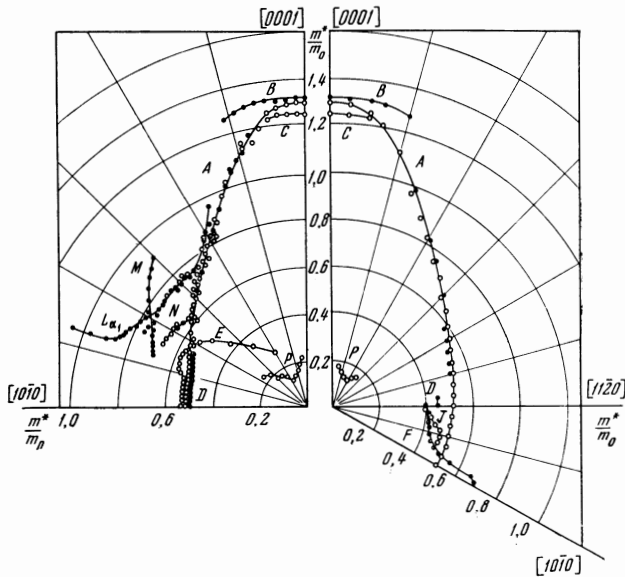


FIG. 3. Anisotropy of effective masses in the $(11\bar{2}0)$, $(10\bar{1}0)$, and (0001) planes. \circ and \bullet are the effective masses for which resonance is observed at $\mathbf{J} \perp \mathbf{H}$ and $\mathbf{J} \parallel \mathbf{H}$, respectively.

squares, to determine how well this part of the surface can be described by a sphere. It was found that within the angular interval extending to $\pm 20^\circ$ from the $[0001]$ axis a lens is well approximated by a sphere with the radius $R = 1.36 \text{ \AA}^{-1}$ measured from a center separated by the distance $\rho = 1.10 \text{ \AA}^{-1}$ from the center of the lens. The radius of curvature of this part of the surface was also determined from the size effect at the limiting point,^[14] the result was $R = 1.32 \pm 0.1 \text{ \AA}^{-1}$. By comparison, in the free electron model we have $R_{\text{fr.e.}} = 1.406 \text{ \AA}^{-1}$ and $\rho_{\text{fr.e.}} = 1.132 \text{ \AA}^{-1}$.

An investigation of the size effect in an oblique field^[14] showed that although a lens is a smooth surface, on some of its cross sections the extremum $(\partial S / \partial k_H)_{\text{ext}} = 1.12 \pm 0.03 \text{ \AA}^{-1}$ is reached, where k_H is the projection of the electron wave vector on the magnetic field direction and S is the cross sectional area in the intersecting plane $k_H = \text{const}$.

The anisotropy of the effective mass on the central cross section of the lens is shown in Fig. 3 (denoted by A). The resonances corresponding to the mass A are most intense for $\mathbf{J} \perp \mathbf{H}$. In the angular interval $10\text{--}40^\circ$ from the $[0001]$ axis they also become observable for $\mathbf{J} \parallel \mathbf{H}$ (Fig. 3).

When \mathbf{H} is parallel to the hexagonal axis these resonances are greatly weakened; the resonances C become most intense for $\mathbf{J} \perp \mathbf{H}$, while the B resonances become most intense for $\mathbf{J} \parallel \mathbf{H}$ (Fig. 3).

Since for deviations from the axes of symmetry the normal to a lens-shaped surface and, therefore, the velocity do not coincide with the direction of the momentum, the orbit in coordinate space, while remaining a plane, forms an angle with the plane perpendicular to the magnetic field. As a result, on such orbits both cyclotron resonance and the size effect can be observed for both polarizations of the rf current (as was observed experimentally).

The B resonances are observed only for $\mathbf{J} \parallel \mathbf{H}$ and pertain to limiting points on the spherical cap of a lens. When the field forms an oblique angle with the sample surface these resonances are split and their period is doubled, as is characteristic of resonance at a reference point.

Since the effective mass at a limiting point is $m_{\text{lim}}^* = 1/v\sqrt{K}$ (where v is the electron velocity equalling the Fermi velocity, and K is the Gaussian curvature that is equal in our case to R^{-2}), we can easily obtain the Fermi velocity at the $[0001]$ axis. For $m_{\text{lim}}^* = (1.32 \pm 0.03)m_0$ we have $v_F = (1.05 \pm 0.10) \times 10^8 \text{ cm/sec}$. (In the model we obtain $v_F(\text{fr.e.}) = 1.63 \times 1.63 \times 10^8 \text{ cm/sec}$.)

It is noteworthy that for $\mathbf{H} \parallel [0001]$ the effective mass B at a limiting point somewhat exceeds A on the central cross section. This is possible in only two cases—either when the mass is minimal with respect to k_H on the central cross section and increases monotonically with k_H , or when the mass is maximal for $k_H = 0$ and one additional minimum of $m^* = m(k_H)$ exists between the central cross section and the limiting point, along with the corresponding resonance.

The second possibility can be understood on the basis of the following simplified considerations. Let us assume that the true Fermi surface is found to be nearly an ellipsoid due to distortions of spherical segments. Equal-energy surfaces close to the Fermi surface should, of course, be less distorted and resemble spherical segments more closely. Then the difference between the cross sectional areas of the ellipsoid and sphere in the plane $k_H = \text{const}$ should be characterized by a function $m^* = m(k_H)$. With these assumptions the areal difference is defined by $m^* \sim \Delta S = ak_H^2 + bk_H$, where $a > 0$. This function actually describes a parabola with its minimum given by $k_H = b/2a$. A similar situation should exist for other directions of the magnetic field, especially when \mathbf{H} is parallel to a twofold axis of symmetry. Experiment has actually revealed C and D resonances close to the $[0001]$, $[10\bar{1}0]$, and $[11\bar{2}0]$ directions; the corresponding masses are close to the A mass and ex-

hibit anisotropy similar to that of the latter.²⁾

The effective C mass is, as would be expected, smaller than the A mass on the central section, and is smaller than the B mass at a limiting point. It may seem strange at first that the corresponding resonance is observed only for $\mathbf{J} \perp \mathbf{H}$. But it will become clear from what follows that precisely this polarization should be predominant. The D resonance is observed for $\mathbf{J} \parallel \mathbf{H}$ only when there are no other resonances with close masses. It remains possible that the C and D resonances could be observed at intermediate angles and possibly merge. However, the spectral complexity in this region resulting from the presence of other resonances does not permit reliable discrimination. A confirmation of this interpretation would have been resonance line shapes indicating mass maxima or minima.

The analysis of line shape is greatly hindered by other resonances, and reliable data can be obtained only for the A resonance near $[10\bar{1}0]$. This resonance is marked by clear asymmetry of the line of dR/dH , which corresponds to $m^*(k_H) = m_{\max}$.^[15] The intensity of the D resonances depends very strongly on the inclination of the field to the surface of the sample. This is especially prominent in the $(10\bar{1}0)$ plane, where resonance disappears for $\sim 10^\circ$ inclination of the field. This result indicates that there is a large component of the mean velocity \bar{v}_H along the field and confirms the idea that the D resonances pertain to cross sections with no areal extremum that are located at the edges of the lens.

We were unfortunately unable to detect D resonances in the (0001) plane, evidently because of geometrical peculiarities of the orbits. Indeed, in this plane electrons enter the skin layer at considerably larger angles to the surface than in other planes; consequently, the interaction in the rf field is weakened so much that even resonance in the central section appears much weakened. However, some difference between the D masses in the $(10\bar{1}0)$ and $(11\bar{2}0)$ planes ($0.49 m_0$ and $0.45 m_0$) possibly indicates that the lenses along the $[11\bar{2}0]$ and $[10\bar{1}0]$ directions are not completely identical.

If this interpretation of the C and D resonances is correct and they occur on cross sections at the edges of the lenses, we can understand why in the cyclotron resonance experiment D is observed mainly for $\mathbf{J} \parallel \mathbf{H}$, and the C resonance for $\mathbf{J} \perp \mathbf{H}$. In fact, for $\mathbf{H} \parallel [0001]$ cross sections with an extremal mass should be close to the central section and have a relatively small velocity \bar{v}_H , whereas for \mathbf{H} along a twofold axis \bar{v}_H should be large.

THE FERMI SURFACE IN THE SECOND ZONE

The experimental diameters that we assign to the Fermi surface in the second zone are denoted in Fig. 2 by H, H', L_{α_1} , L_{α_2} , L'_{β_2} , and L_{α_3} . In a magnetic field $\mathbf{H} \parallel [0001]$ we observe a quite strong H line, which when the field departs from this direction is split into the two lines H and H'. The most probable interpretation of the H orbit is the neck of the monster on the horizontal face of the zone. The deviation of the field from $[0001]$ leads to extreme complexity of this orbit, which acquires two unidentical maximal diameters. In the course of several electronic orbital circuits only the very largest diameter should have been manifested, because when the smaller diameter equals the plate thickness the orbit should have been cut off. However, as has occurred for In,^[16] both diameters are manifested, and the line splits into the two lines H and H'. This result is evidently associated with the fact that the effect is observed when the electron traverses the skin layer only once.

Exactly the same kind of splitting occurs in the case of the L_{β_2} line, which is observed when the angle between \mathbf{H} and $[10\bar{1}0]$ lies between 32° and 10° in the $(11\bar{2}0)$ plane. The L_{β_2} diameter is considerably greater than the height of the zone and corresponds to an elongated orbit passing through two cells of the reciprocal lattice. For the similar L_{α_1} and L_{α_2} orbits, which traverse one and three cells of the reciprocal lattice, respectively, this line splitting is not observed for some reason. The L_{α_1} line disappears sharply for \mathfrak{H} , $[10\bar{1}0] = 16^\circ$, when the corresponding orbit approaches a saddle point. When \mathfrak{H} , $[10\bar{1}0] > 65^\circ$ it is also unobserved. When \mathbf{H} is oriented along $[0001]$ a line appears which we regard preferentially as L_{α_1} . However, we cannot prove this interpretation. The L_{α_3} line is observed at angles from 11° to 6° . Beginning at 5° the registration of the size effect is very complex, and at 2.5° the size effect is observed for "ineffective" electrons of open cross sections in the form of harmonic oscillations.^[11]

Although the diameters of the H, L_{α_1} , L_{α_3} , and

²⁾In [7] the C resonance is ascribed to orbits on the monster, based on the assumption that the small gap is constricted at its middle to produce a closed orbit traversing three fragments of the monster. We regard this as a less likely interpretation. According to data in [8] the C mass exceeds the A mass but is smaller than the B mass. The C and D masses are also interpreted as being located on noncentral sections of a lens.

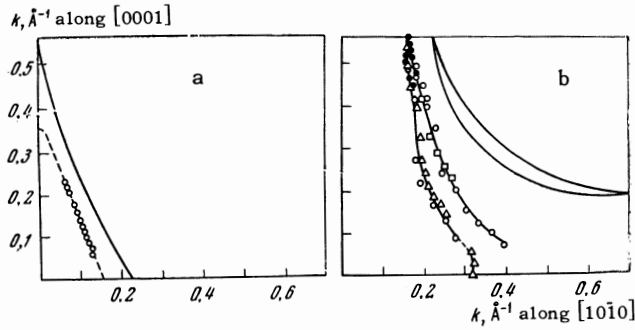


FIG. 4. Projections of a part of (a) pyramids and (b) monster on the $(11\bar{2}0)$ plane; the solid curves are projections in the almost free electron model. In Fig. 4b the different points designate experimental radii of the H, H', L_{α_1} , L_{β_2} , L_{β_2}' , and L_{α_3} orbits, plotted from different points on the ordinate axis: \bullet —H and H', Δ — L_{α_1} , \circ — L_{β_2} and L_{β_2}' , \square — L_{α_3} .

L_{β_2} orbits are not identical they actually represent almost identical projected parts of the Fermi surface in the $(11\bar{2}0)$ plane. Figure 4b shows the anisotropy of the diameters of all these orbits when their centers are located at different points of the Brillouin zone. Thus, the diameter of the L_{α_1} orbit was plotted at the coordinate origin, for H and H' at the point $+d/2$ on the ordinate axis, for L_{β_2} and L_{β_2}' at the point $-d/2$, and for L_{α_3} at the point $-d$ (where d is the height of the Brillouin zone). We observe the good fit of all points on two curves representing the Fermi surface projection. In the figure the projection in the almost free electron model is also shown.

The plotting of the projection in the $(10\bar{1}0)$ plane is considerably more difficult, because the projection has no center of symmetry in this plane. Nevertheless, the identification of the H, H', and L_{α_1} orbits with similar orbits in the $(11\bar{2}0)$ plane cannot be doubted. A comparison between our data and data based on the de Haas–van Alphen effect is very difficult because we do not know the exact shapes of the extremal cross sections and can calculate their areas only approximately. If, for example, we assume that the cross section of the neck of the monster is an equilateral triangle the area of its cross section is $S = 0.047 \text{ \AA}^{-2}$. From de Haas–van Alphen data $S = 0.0535 \text{ \AA}^{-2}$ with 5% accuracy; it is here 15% larger. From the de Haas–van Alphen effect we obtain $S = 0.193 \text{ \AA}^{-2}$ for the cross sectional area of one part of the monster in its broadest part ($\gamma^{1/3}$ in ^[4]). Our data, if the cross section is assumed to be a triangle whose height equals its base, give $S = 0.205 \text{ \AA}^{-2}$.

Orbits traversing one, two, three etc. zones on the monster are also observed in cyclotron resonance. Since the monster can be represented as a

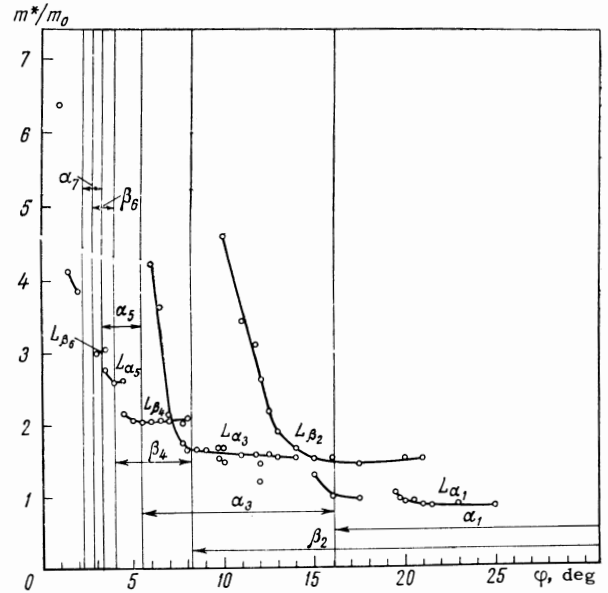


FIG. 5. Angular dependences of the effective masses for L_{α_n} and L_{β_n} in the $(11\bar{2}0)$ plane; the corresponding orbits traverse several zones. The vertical lines bound the ranges α_n and β_n within which such orbits can exist according to size effect data. $\varphi = 0$ for $\mathbf{H} \parallel [10\bar{1}0]$; $\mathbf{J} \parallel \mathbf{H}$.

corrugated cylindrical surface, the angular dependence of the mass, $m^* \sim 1/\sin \varphi$, as required for a right cylinder, must be subjected to sharp changes associated with the existence of saddle points, where self-intersecting orbits appear. When an orbit approaches such a point the effective mass must be greatly increased, while vanishing at the saddle point.^[17]

A very similar pattern is observed experimentally for $\mathbf{J} \parallel \mathbf{H}$. Figure 5 shows the anisotropy of the effective masses for L_{α_n} and L_{β_n} in the $(11\bar{2}0)$ plane; the corresponding orbits traverse several zones. The angular limits are shown for the existence of the orbits according to size effect data. In the immediate vicinity of the $[10\bar{1}0]$ direction, the inaccuracy of its orientation (of the order of one degree) made it difficult to assign an effective mass to any particular zone. However, at 3° or 4° from the given direction the correspondence with the numerical designations of the zones becomes more apparent. This pertains especially to the L_{β_2} and L_{α_3} masses, for which we observe steep growth when the orbit approaches a saddle point. There is a clear general tendency for mass increase as the given orientation is approached, as would be required for a cylinder. It is interesting that the mass for a given zone remains practically constant, excluding the immediate vicinity of the saddle point.

For the L_{α_1} mass, which is shown on a larger

scale in Fig. 3, some increase is also observed, although the corresponding resonances disappear at $\varphi = 19.5^\circ$ for some reason. This is strange because for the L_{α_3} mass resonance is observed in the cases of orbits passing considerably closer to the saddle point.

Beginning at $\varphi \approx 40^\circ$ from the given direction, resonance corresponding to the L_{α_1} mass is also observed for $\mathbf{J} \perp \mathbf{H}$ polarization. With increase of the angle the mass size approaches that for A. This resonance is not observed for angles exceeding 57° .

In the plane (0001) for both polarizations of the rf current cyclotron resonance is observed corresponding to the F mass in Fig. 3. In two other planes both the angular interval and intensity are very small. The most appropriate orbit would pass along external and internal parts of one fragment of the monster, as shown in Fig. 1.

In addition to the quite well interpreted effective masses several resonances are observed for which it is difficult to designate the orbits. These include especially the M and N masses observed in the angular intervals $19.5^\circ - 44^\circ$ and $23^\circ - 38^\circ$ from [1010]. The abrupt disappearance of the corresponding resonances at almost the same angles as for the L_{α_1} resonances suggests that the orbits are located on some non-central sections of the monster. The possible existence of these cross sections is also indicated by the appearance of additional resonances at 10° , 12° , and $15^\circ - 17^\circ$, where the orbits pass through two or three zones; it is also difficult to interpret these cases on the basis of central sections.

THE PYRAMID-SHAPED SURFACE IN THE FIRST ZONE

In the planes $(10\bar{1}0)$ and $(11\bar{2}0)$ we observe a quite intense size effect line P within the angular (φ) intervals $90^\circ - 17^\circ$ and $65^\circ - 16^\circ$ ($\varphi = 0$ for $\mathbf{H} \perp [0001]$). The orbital diameter given by this line and the character of the anisotropy cause it to be assigned to a pyramid in the first zone. Figure 4a shows the diameter of the P orbit and the neck of the monster in the $(11\bar{2}0)$ plane, where the projection of the pyramid is symmetrical. This figure also shows the projection in the almost free electron model; all the points are seen to fit well on a straight line. Projection on the $[10\bar{1}0]$ direction gives a diameter very close to that of the neck of the monster. Projection on $[0001]$, taking into account the rounding off of the vertex that was observed at 2° according to the de Haas-van Alphen effect,^[14] shows that the vertex of a pyramid fails

by about $0.2 - 0.17 \text{ \AA}^{-1}$ to reach the point K of the Brillouin zone (Fig. 1).

In the planes $(10\bar{1}0)$ and $(11\bar{2}0)$, for $\mathbf{J} \perp \mathbf{H}$ cyclotron resonance is observed with a small mass; the designation in Fig. 3 is P. This resonance is very sensitive to the angle between \mathbf{J} and \mathbf{H} ; the resonance disappears when this angle differs by $10^\circ - 15^\circ$ from a right angle. The small effective mass and the anisotropy with its minimum for $\mathbf{H}, [0001] \approx 30^\circ$ suggest that this mass belongs to orbits on a pyramid.

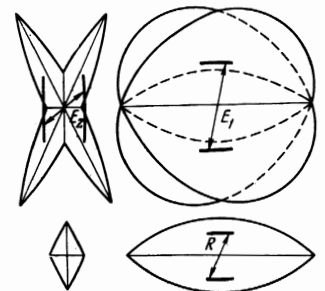
THE THIRD-ZONE STAR-SHAPED AND FOURTH-ZONE CIGAR-SHAPED SURFACES

In magnetic fields up to 100 Oe a few additional relatively weak size-effect lines are observed. The corresponding diameters are so small that they can hardly be ascribed to the monster, and even less easily to a lens. Since the numbers of electrons and holes are equal in cadmium, for an almost unchanged lens volume and greatly reduced monster volume we can expect that the remaining Fermi electron surfaces given by the almost free electron model should be greatly reduced in size and apparently distorted. Therefore all small extremal diameters as functions of the anisotropy can be assigned preferentially to star or cigar surfaces.

Figure 6 shows a possible interpretation of some of these diameters in the $(11\bar{2}0)$ plane, where the projections are symmetrical. If we interpret these small diameters correctly it seems strange that these types of surfaces are not observed through the de Haas-van Alphen effect, where they should yield small cross-section areas. The data obtained regarding these Fermi surfaces are too sparse to permit reliable conclusions about their shapes. However, it is evident that such surfaces exist, and their shapes and diameters differ greatly from the values given by the almost free electron model.

In the $(11\bar{2}0)$ plane, for $\mathbf{J} \perp \mathbf{H}$ cyclotron resonance is observed corresponding to the effective mass E in Fig. 3. Although this resonance is very weak against the background of the A resonance,

FIG. 6. A possible interpretation of the small diameters E_1 , E_2 , and R in the $(11\bar{2}0)$ plane. The fine lines represent projections of stars and cigars in the almost free electron model; the heavy lines represent experimental results.



its anisotropy can be traced. The angular dependence of the E mass very much resembles the shape of a star with greatly smoothed prongs. Unfortunately, the cyclotron resonance data are also fragmentary and do not permit reliable conclusions.

CONCLUSIONS

The following conclusions are based on the investigation of the Fermi surface of cadmium by means of the rf size effect and cyclotron resonance:

1. The almost free electron model of the Fermi surface with spin-orbit splitting taken into account can be used as a first approximation for the interpretation of experimental data if we permit very considerable modifications of the model by the lattice potential.

2. The best agreement with the model (with regard to both shape and diameter) is obtained for lenses in the third zone. This type of surface is smooth and resembles an oblate ellipsoid of rotation. However, the dispersion law for this surface is not quadratic. Moreover, the effective mass appears to have an extremum at the edges as well as in the central section of the surface. As in the model, a lens has cross sections with the extremal quantity $(\partial S/\partial k_H)_{\text{ext}}$. The middle of a lens resembles a spherical cap on which there is little variation of the radius of curvature and effective mass, and consequently of the Fermi velocity.

3. The hole surface (monster) in the second zone is considerably smaller than in the model, although the overall shapes (with broken arms along $[11\bar{2}0]$) are very similar. The size-effect shape and size of the monster that are associated with additional assumptions regarding the shapes of extremal cross sections are consistent with the de Haas-van Alphen effect. The experimental cyclotron resonance results confirm that the monster is a surface that is open along $[0001]$ and that it is a corrugated cylinder. The angular intervals where we observe effective masses on orbits passing through several zones are in good agreement with the corrugation parameters obtained from the size effect.

4. Pyramid-like surfaces in the first zone also resembled the model in shape but were somewhat smaller. This type of surface exhibits cyclotron resonance with an effective mass having its minimum for χ_H , $[0001] \approx 30^\circ$, like the cross-sectional area in the de Haas-van Alphen effect.

5. Small measured orbital diameters were assigned preferentially to star surfaces in the third zone and cigar surfaces in the fourth zone. Cyclotron resonance here also gives an effective mass whose anisotropy resembles that of a star with greatly smoothed prongs. However, the incompleteness of these data prevents definite conclusions concerning the shapes of these surfaces.

In conclusion we wish to thank B. N. Aleksandrov for providing a bar of pure cadmium, V. I. Konovalova and B. A. Stebletsov for preparing samples, and I. Kh. Albegova, I. P. Okhrimenko, and É. I. Ol'khovskii for experimental assistance.

¹N. E. Alekseevskii and Yu. P. Gaïdukov, JETP 43, 2094 (1962), Soviet Phys. JETP 16, 1481 (1963).

²A. S. Joseph, W. L. Gordon, J. R. Reitz, and T. G. Eck, Phys. Rev. Letters 7, 334 (1961).

³A. D. C. Grassie, Phil. Mag. 9, 847 (1964).

⁴D. C. Tsui and R. W. Stark, Phys. Rev. Letters 16, 19 (1966).

⁵M. R. Daniel and L. Mackinnon, Phil. Mag. 8, 537 (1963).

⁶D. F. Gibbons and L. M. Falicov, Phil. Mag. 8, 177 (1963).

⁷J. K. Galt, F. R. Merritt, and J. R. Klauder, Phys. Rev. 139, A823 (1965).

⁸M. P. Shaw, T. G. Eck, and D. A. Zych, Phys. Rev. 142, A406 (1966).

⁹W. A. Harrison, Phys. Rev. 118, 1190 (1960).

¹⁰J. D. Gavenda and B. C. Deaton, Phys. Rev. Letters 8, 208 (1962).

¹¹A. A. Mar'yakhin and V. P. Naberezhnykh, Pis'ma JETP 3, 205 (1966), JETP Letters 3, 130 (1966).

¹²Yu. A. Bartashevskii and A. N. Otko, PTÉ No. 4, 250 (1965).

¹³Yu. V. Sharvin and V. G. Gantmakher, PTÉ No. 6, 1965 (1963).

¹⁴V. P. Naberezhnykh and A. A. Mar'yakhin, Phys. Status Solidi 20, No. 2 (1967).

¹⁵R. G. Chambers, Proc. Phys. Soc. (London) 86, 305 (1965).

¹⁶V. F. Gantmakher and N. P. Krylov, JETP 49, 1054 (1965), Soviet Phys. JETP 22, 734 (1964).

¹⁷I. M. Lifshitz and M. I. Kaganov, UFN 69, 419 (1959), Soviet Phys. Uspekhi 1, 831 (1960).